JPn Neuroscience
The Journal of Physiology

Synaptic transmission at the endbulb of Held deteriorates during age-related hearing loss

Ruili Xie[1] and Paul B. Manis[2,3]

[1] *Department of Neurosciences, University of Toledo, Toledo, OH 43614-2598, USA*
[2] *Department of Otolaryngology/Head and Neck Surgery, The University of North Carolina at Chapel Hill, Chapel Hill, NC 27599-7545, USA*
[3] *Department of Cell Biology and Physiology, The University of North Carolina at Chapel Hill, Chapel Hill, NC 27599-7070, USA*

Key points

- Synaptic transmission at the endbulb of Held was assessed by whole-cell patch clamp recordings from auditory neurons in mature (2–4 months) and aged (20–26 months) mice.
- Synaptic transmission is degraded in aged mice, which may contribute to the decline in neural processing of the central auditory system during age-related hearing loss.
- The changes in synaptic transmission in aged mice can be partially rescued by improving calcium buffering, or decreasing action potential-evoked calcium influx.
- These experiments suggest potential mechanisms, such as regulating intraterminal calcium, that could be manipulated to improve the fidelity of transmission at the aged endbulb of Held.

Abstract Age-related hearing loss (ARHL) is associated with changes to the auditory periphery that raise sensory thresholds and alter coding, and is accompanied by alterations in excitatory and inhibitory synaptic transmission, and intrinsic excitability in the circuits of the central auditory system. However, it remains unclear how synaptic transmission changes at the first central auditory synapses during ARHL. Using mature (2–4 months) and old (20–26 months) CBA/CaJ mice, we studied synaptic transmission at the endbulb of Held. Mature and old mice showed no difference in either spontaneous quantal synaptic transmission or low frequency evoked synaptic transmission at the endbulb of Held. However, when challenged with sustained high frequency stimulation, synapses in old mice exhibited increased asynchronous transmitter release and reduced synchronous release. This suggests that the transmission of temporally precise information is degraded at the endbulb during ARHL. Increasing intraterminal calcium buffering with EGTA-AM or decreasing calcium influx with ω-agatoxin IVA decreased the amount of asynchronous release and restored synchronous release in old mice. In addition, recovery from depression following high frequency trains was faster in old mice, but was restored to a normal time course by EGTA-AM treatment. These results suggest that intraterminal calcium in old endbulbs may rise to abnormally high levels during high rates of auditory nerve firing, or that calcium-dependent processes involved in release are altered with age. These observations suggest that ARHL is associated with a decrease in temporal precision of synaptic release at the first central auditory synapse, which may contribute to perceptual deficits in hearing.

(Received 20 April 2016; accepted after revision 7 September 2016; first published online 13 September 2016)
Corresponding author R. Xie, PhD: 186 Block Health Science Building, MS1007, Department of Neurosciences, University of Toledo, 3000 Arlington Avenue, Toledo, OH 43614-2598, USA. Email: ruili.xie@utoledo.edu

Abbreviations ABR, auditory brainstem response; ACSF, artificial cerebrospinal fluid; ARHL, age-related hearing loss; eEPSC, evoked excitatory postsynaptic current; N_{min}, lower limit of release sites; P_r, initial release probability; sEPSC, spontaneous excitatory postsynaptic current; PPR, paired pulse ratio; RRP, readily releasable pool; SGC, spiral ganglion cell.

DOI: 10.1113/JP272683

Introduction

Hearing impairment is a common occurrence amongst the elderly, and occurs as a gradual decline in auditory function referred to as age-related hearing loss (ARHL). It is well known that the auditory periphery undergoes structural changes during ageing, including a loss of hair cells (Bohne *et al.* 1990), a loss of synaptic connections between the hair cells and the spiral ganglion cells (SGCs) (Hequembourg & Liberman, 2001; Sergeyenko *et al.* 2013; Viana *et al.* 2015), and functional changes such as a decrease in the endocochlear potential (Schulte & Schmiedt, 1992). These peripheral changes lead to decreased sensory input into the central auditory system, and are widely accepted as leading proximal causes of ARHL. However, auditory information is further processed in the CNS, which also has been shown to exhibit its own age-related functional and structural changes. In the elderly, central processing deficits are thought to underlie a compromised ability to process the fine temporal structure of sound (Lorenzi *et al.* 2006; Anderson *et al.* 2012), and impair sound detection in noisy environments (Frisina & Frisina, 1997). Although age-related changes in sensory processing have been well documented (Caspary *et al.* 2005; Wang & Manis, 2005; Frisina & Walton, 2006), many of the cellular mechanisms that contribute to ARHL remain unexplored.

The endbulb of Held synapse is the first synaptic contact between the SGCs of the auditory nerve and the bushy neurons of the cochlear nucleus. The bushy cells are specialized to encode the temporal information of sound for further processing at higher levels of the auditory system (Manis *et al.* 2011), including timing cues in the tens to hundreds of microseconds that are utilized by higher auditory structures for azimuthal sound localization (Joris & Yin, 2007) and pitch identification (Shofner, 2008). The endbulb of Held has been widely used to study aspects of synaptic transmission (Manis *et al.* 2011), but the majority of these studies have been limited to juvenile animals. Given that the processing of fine temporal structure is compromised during ARHL (Anderson *et al.* 2012), we hypothesized that the ability of the endbulb of Held synapses to transmit temporal cues decreases during ageing.

Using brain slices from CBA/CaJ mice, we found that at low stimulus rates, endbulb of Held synapses show normal transmitter release in mature and old mice. However, at high stimulus rates, endbulb of Held synapses in old mice have decreased phasic release and elevated asynchronous release. In old mice, the degraded transmission appears to be associated with calcium-dependent processes in the endbulb synapse, because either the addition of an exogenous calcium buffer or a decrease in action potential-evoked calcium influx could restore phasic release when challenged at high stimulus rates. The decreased phasic release is expected to result in poor transmission of information about the fine temporal structure of sounds to the central auditory pathways.

Methods

Ethical approval

All experiments were carried out under the guideline of the protocols approved by the Institutional Animal Care and Use Committee at the University of North Carolina at Chapel Hill (UNC-CH) and the University of Toledo (UT).

Animals

CBA/CaJ mice of either sex at ages of 2–4 months (mature; 19 female, 13 male) and 20–26 months (old; 12 female, 3 male) were used. The CBA/CaJ strain was chosen in this study because these mice do not carry any known mutations of hearing loss, show stable hearing through adulthood (Zheng *et al.* 1999), but go on to develop ARHL at old ages during natural ageing (Sergeyenko *et al.* 2013). This pattern of hearing progression closely mimics the development of ARHL in humans. Mice were housed in animal facilities with enriched environments. The mature mice were maintained on a Harlan diet through their lifetime. The old mice spent the first 14 months of their life on a Purina diet, but were then switched to the Harlan diet by the UNC Division of Laboratory Animal Medicine. Experiments performed at UT used five old mice transferred from UNC-CH and eight mature mice that were bred on site at the UT Health Science Campus, where only the Harlan diet was used.

Auditory brainstem response (ABR)

Mice were anaesthetized with ketamine (100 mg kg^{-1}) and xylazine (10 mg kg^{-1}) via intraperitoneal injection, and placed on a feedback-controlled heating pad in a sound attenuating box to measure ABRs as previously described (Xie & Manis, 2013*a*). For ABR recordings made at UNC-CH, clicks (10 μs pulse duration, monophasic) were generated by a high-speed 16-bit DAC (National Instruments NI6731; Austin, TX, USA), attenuated and amplified (Tucker Davis PA5 attenuator and SA5 amplifier; Alachua, FL, USA), and delivered by a free-field speaker (Tucker Davis, MF1) positioned ~5 cm from the ipsilateral ear. ABR recordings made at UT used an RZ6-A-P1 bioacoustic system with BioSigRZ software (Tucker Davis). ABRs were recorded between needle electrodes at the pinnae and vertex, with the remote ground over the rump. Stimuli were presented in 5 dB increments over a range 20–80 dB SPL, and responses to a total of 512 stimuli delivered at 40 Hz in 1 s long blocks of 25 alternating

condensation and rarefaction polarity were averaged after artifact rejection, using a custom MATLAB program. The visually determined ABR thresholds and the negative to positive peak amplitudes of the first ABR wave were used to assess hearing status (Fig. 1).

Brain slice preparation

Following ABR measurement, mice were given a supplemental dose of the same ketamine/xylazine cocktail, and decapitated. The brainstem was removed and transferred into artificial cerebrospinal fluid (ACSF) at 34°C, gassed with 5% CO_2 and 95% O_2. Parasagittal slices (350 μm) containing the cochlear nucleus were cut with a Vibratome 1000 (Technical Products, Inc., Hubertus, WI, USA) (Xie & Manis, 2013*b*, *a*). Slices were bathed in ACSF at 34°C for 30 min, and transferred to a submersion chamber on a fixed-stage FS2 (UNC-CH) or an Axio Examiner (UT) microscope (Zeiss, Oberkochen, Germany) for recordings, which were also performed at 34°C. The ACSF contained (in mM): 122 NaCl, 3 KCl, 1.25 NaH_2PO_4, 25 $NaHCO_3$, 20 glucose, 3 *myo*-inositol, 2 sodium pyruvate, 0.4 ascorbic acid, 2.5 $CaCl_2$ and 1.5 $MgSO_4$. Inhibitory synaptic transmission was blocked in all recordings with 2 μM strychnine in ACSF.

Data acquisition

Data acquisition was performed with the program ACQ4 (Campagnola *et al.* 2014) at UNC-CH, or pClamp10 software at UT. Voltage clamp recordings were made from bushy neurons in the anteroventral cochlear nucleus as previously reported (Xie & Manis, 2013*a*,*b*), using a Multiclamp 700B amplifier (Axon Instruments, Union City, CA, USA) with 75% compensation in a 15 kHz bandwidth; recordings were low-pass filtered at 6 kHz and digitized at 50 kHz. The recording pipette was pulled from borosilicate glass (KG-33; King Precision Glass, Claremont, CA, USA) using a Sutter P-2000 puller (Sutter Instruments, Novato, CA, USA), with a resistance of 3–5 MΩ. Data were acquired from neurons with access resistance less than 15 MΩ. The recording pipette contained (in mM): 130 $CsMetSO_3$, 5 CsCl, 5 EGTA, 10 Hepes, 4 MgATP, 0.3 Tris-GTP, 10 Tris-phosphocreatine, and 3 QX-314, pH adjusted to 7.2 with CsOH. Bushy cells were identified morphologically during the experiment by including Alexa Fluor 488 (Molecular Probes, Carlsbad, CA, USA) in the pipette solution and imaging the cell's fluorescence at the end of the recording session. Cells were held at −68 mV (corrected with a junction potential of −8 mV). A 75 μm diameter concentric stimulating electrode (Fredrick Haer Company, Bowdoinham, ME, USA) was placed in the auditory nerve root to evoke excitatory postsynaptic currents (eEPSCs) in bushy neurons. Stimuli were 100 μs pulses delivered through an analog stimulator in constant current mode (Dagan Cornerstone S910 and S940). EGTA-AM (Life Technologies, Carlsbad, CA, USA) was made as a 100 mM stock in DMSO (Sigma-Aldrich, St Louis, MO, USA) and diluted to a final concentration of 100 μM in ACSF for each use. To load cells and synapses with EGTA-AM, slices were incubated in ACSF containing EGTA-AM at room temperature for 10 min, and then returned to standard ACSF at 34°C for 15 min before commencing recording. The P-type calcium channel blocker ω-agatoxin IVA (Alomone Labs, Jerusalem, Israel) was bath-applied at 25 nM.

Spontaneous EPSCs (sEPSCs) were detected and analysed with a custom program in MATLAB using the scaled template method (Clements & Bekkers, 1997). All

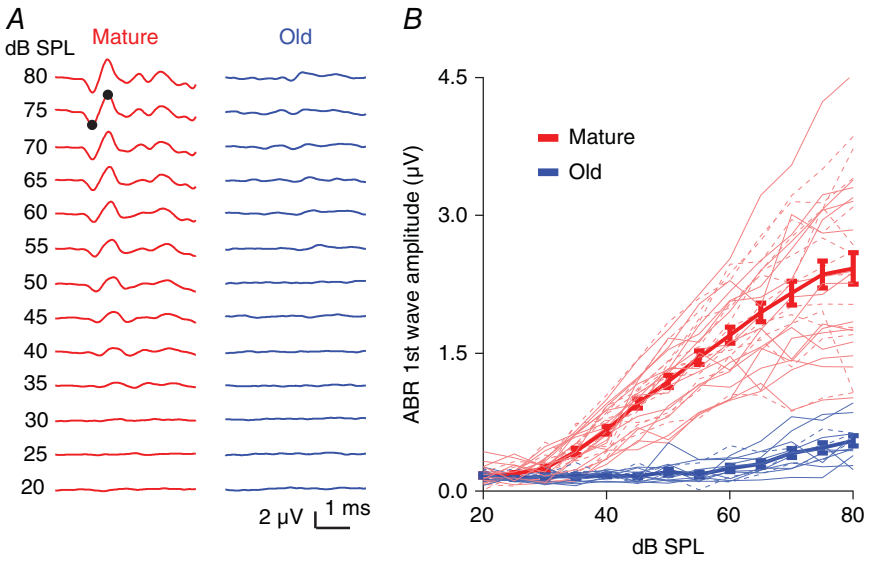

Figure 1. CBA/CaJ mice show ARHL
A, example ABR waveforms recorded from mature and old mice in response to clicks. Black dots mark the rising phase and peak of the first wave. *B*, growth curve of the ABR first wave amplitude for increasing click intensity. Thick lines are averages of all mice in each group (error bars are SEM). Thin lines show individual mice; continuous lines: female; dashed lines: male.

other analyses used custom programs in Igor Pro (V6.0, WaveMetrics, Inc., Lake Oswego, OR, USA).

Variance-mean analysis

Variance-mean analysis was used to assess the initial release probability (P_r) and to estimate a lower limit of independent release sites (N_{min}) (Reid & Clements, 1999; Oleskevich *et al.* 2000; Wang & Manis, 2005) (Fig. 3). Single eEPSCs were recorded in different P_r conditions obtained by adjusting the calcium concentration (1, 2 and 3 mM) of the external ACSF as previously described (Wang & Manis, 2005). The mean eEPSC amplitude and the variance under each P_r condition were obtained from stable recordings of 50–100 single eEPSCs with less than 20% drift. Because different calcium concentrations were used in this set of experiments, the acquired data were only used for the variance-mean analysis shown in Fig. 3 and were not included in other analyses. The variance-mean data were fit to a parabola that goes through the origin with the equation: $y = Ax + Bx^2$, where y is eEPSC variance and x is eEPSC mean amplitude. P_r was calculated as: $P_r = x(-B/A)(1+CV^2)$, where the CV (coefficient of variation) was calculated from eEPSCs evoked in the same neuron. A lower limit for the number of release sites at the synapse was then estimated as: $N_{min} = -1/B$.

Statistics

Prism 6.0 (GraphPad Software Inc., La Jolla, CA, USA) was used for all statistical tests except in Fig. 2*I*. Paired and unpaired Student's *t* test (or Mann–Whitney test when the data population failed to pass the normality test), one-way ANOVA as well as two-way ANOVA were used as stated. To test whether paired-pulse ratios (PPRs) were different between ages (Fig. 2*I*), we used a linear mixed effects model (package lme4 in R, V3.3.1) because, for some cells, not all time intervals had been tested as required for a standard two-way repeated-measures ANOVA. Data are presented as mean and standard deviations (SD), except in Figs 1*B*, 3*F*, 4*E*, *G* and *J*, 6*E*, *F*, and 7*C*, *D* as specified, where the data are presented as mean ± standard error of the mean (SEM) to minimize trace overlap.

Results

ARHL in old CBA/CaJ mice

We evaluated the hearing status of the CBA/CaJ mice by measuring click-evoked ABRs from 20 to 80 dB SPL. Compared to mature mice (2–4 months), old mice (20–26 months) showed an ARHL characterized by a significantly elevated ABR threshold [Fig. 1*A*; mature:

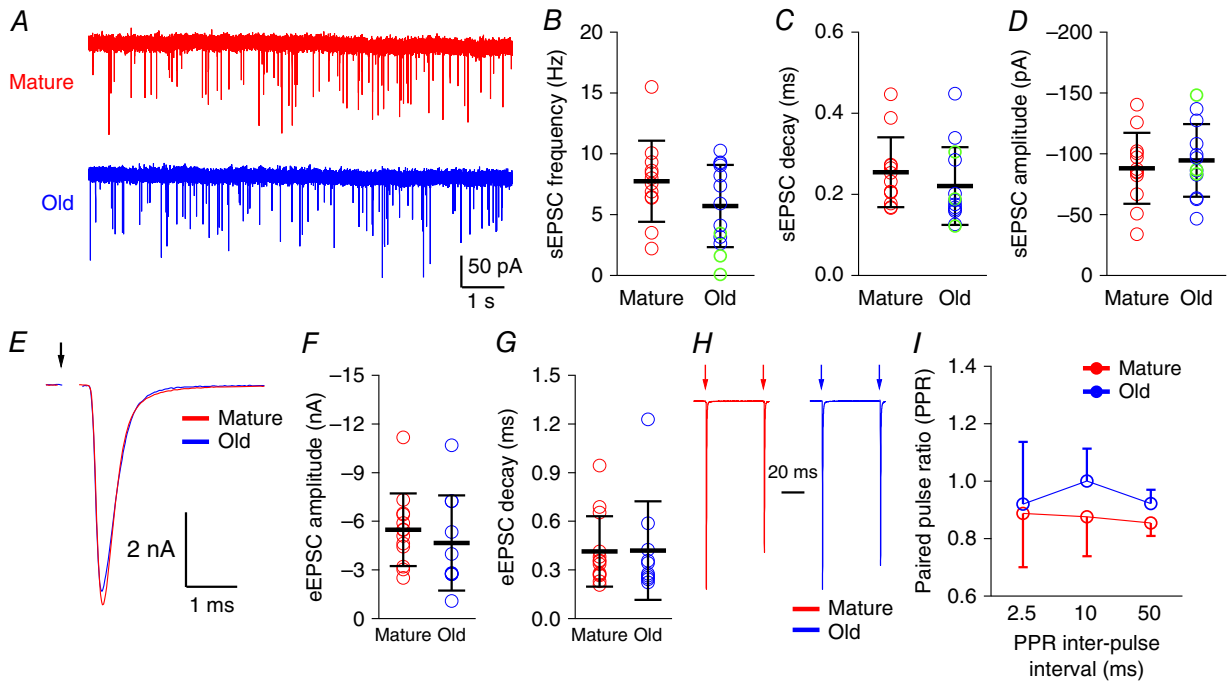

Figure 2. Synaptic transmission at the endbulb of Held in mature and old mice
A, spontaneous EPSCs in bushy neurons in mature and old mice. *B–D*, summary for all bushy neurons in mature and old mice. *B*, sEPSC frequency; *C*, sEPSC decay time constant; *D*, average sEPSC amplitude. Circles: individual cells; red: cells from mature mice; blue: cells from old mice with evoked EPSCs; green: cells ($n = 3$) from old mice where stimulation failed to evoke eEPSCs. *E*, eEPSCs from mature and old mice. Arrow: stimulus onset. *F* and *G*, summary data for eEPSC amplitude (*F*) and decay time constant (*G*). *H*, example normalized paired-pulse eEPSCs with 50 ms interval from mature and old mice. *I*, summary of PPR. Data are presented as mean ± SD.

32 dB SPL (SD 5, $n = 29$); old: 56 dB SPL (SD 10, $n = 13$); unpaired t test: $t_{40} = 10.52$, $P < 0.0001$]. Above 40 dB SPL, the amplitude of the first ABR wave was also significantly smaller in old mice (Fig. 1*B*; two-way ANOVA, age effect: $F_{1, 518} = 660.8$, $P < 0.0001$; sound intensity effect: $F_{12, 518} = 50.52$, $P < 0.0001$; interaction: $F_{12, 518} = 28.62$, $P < 0.0001$; Sidak's multiple comparisons test: $P < 0.0001$ for wave amplitudes at all levels above 45 dB SPL, $P < 0.01$ at 40 dB SPL). This is consistent with previous reports of ARHL in CBA/CaJ mice (Sergeyenko *et al.* 2013). Differences in hearing status between male and female mice were not observed in either mature (two-way ANOVA, sex effect: $F_{1,351} = 2.80$, $P = 0.0951$) or old (two-way ANOVA, sex effect: $F_{1, 141} = 1.17$, $P = 0.281$) mice. It has been previously reported that male mice develop ARHL earlier than female mice (Guimaraes *et al.* 2004; Henry, 2004); that we found no sex difference is probably due to the small number of male mice in the old group.

Synaptic transmission at the endbulb of Held in mature and old mice

We next assessed the quantal transmission at the endbulb of Held by recording sEPSCs for 100–200 s from each bushy neuron in whole-cell voltage clamp (Fig. 2*A*). The number of sEPSCs in bushy neurons ranged from 19 to 2949 events, with a median of 970 events in mature mice and 822 events in old mice. There was no significant difference between the two age groups for sEPSC frequency [Fig. 2*B*; mature: 7.8 Hz (SD 3.3, $n = 12$); old: 5.7 Hz (SD 3.4, $n = 13$); unpaired t test: $t_{23} = 1.51$, $P = 0.146$], sEPSC decay time constant [Fig. 2*C*; mature: 0.25 ms (SD 0.09, $n = 12$); old: 0.22 ms (SD 0.10, $n = 13$); unpaired t test: $t_{23} = 0.93$, $P = 0.362$] or sEPSC amplitude [Fig. 2*D*; mature: −88 pA (SD 29, $n = 12$); old: −95 pA (SD 30, $n = 13$); unpaired t test: $t_{23} = 0.54$, $P = 0.592$]. Thus, the basic aspects of quantal transmission at the endbulb of Held appear to be largely unchanged during ARHL.

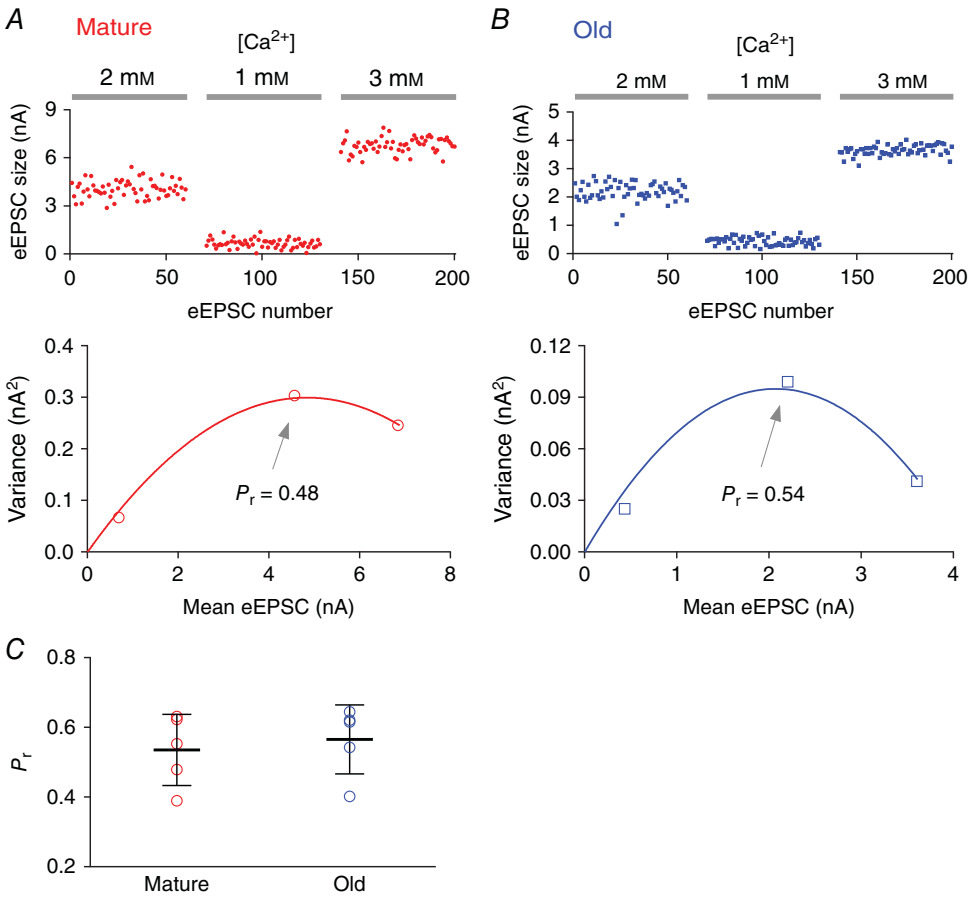

Figure 3. Initial release probability at the endbulb of Held synapses in mature and old mice assessed by variance-mean analysis
A, top: eEPSCs recorded from a bushy neuron of a mature mouse in response to auditory nerve stimulation under different extracellular calcium concentrations. Bottom: variance-mean plot of eEPSCs for the three calcium concentrations. The initial release probability (P_r) at 2 mM [Ca^{2+}] was estimated by fitting the data to a parabola (see Methods). *B*, top: eEPSCs recorded from a bushy neuron from an old mouse. Bottom: variance-mean plot for data in top panel. *C*, summary of release probabilities at 2 mM [Ca^{2+}] in mature and old mice.

We next evaluated how ARHL affects evoked release at the endbulb of Held. In these experiments, the stimulus level was gradually increased until reliable eEPSCs were obtained. This level was then used for all eEPSC recordings in a given cell. All 13 bushy neurons in the mature group of mice responded with eEPSCs with an average stimulation amplitude at 270 μA (SD 170). In the old mice, stimulation produced eEPSCs in 10 of 13 bushy neurons with an average stimulation amplitude of 440 μA (SD 320). The difference in stimulus levels between mature and old mice was not statistically significant (unpaired t test: $t_{21} = 1.55$, $P = 0.135$). In three neurons from old mice, we were unable to obtain any eEPSCs even after the stimulus was increased to a level (2 mA) that was high enough to cause an electrolytic lesion in the tissue.

For all neurons with evoked responses, neither eEPSC amplitudes nor decay time constants were different between mature and old groups [Fig. 2*E*, *F*, amplitude: mature: −5.5 nA (SD 2.2, $n = 13$); old: −4.7 nA (SD 2.9, $n = 10$); unpaired t test: $t_{21} = 0.75$, $P = 0.459$; Fig. 2*G*, decay time constant: mature: 0.42 ms (SD 0.22, $n = 13$); old: 0.42 ms (SD 0.30, $n = 10$); Mann–Whitney test: $P = 0.633$]. We also examined the PPR at 2.5, 10 and 50 ms inter-pulse intervals (Fig. 2*H*). PPRs were not significantly different between mature and old mice (Fig. 2*I*; linear mixed effects model; PPR as the dependent variable, age and interval as the factors, and subject as a random variable; age effect: $t_{39.5} = 1.405$, $P = 0.168$; interval time effect: $t_{42.6} = -0.697$, $P = 0.490$; interaction between age and interval: $t_{43.8} = -0.070$, $P = 0.945$).

To more directly assess changes in release, in a different set of experiment we assessed the initial release probability (P_r) and estimated the minimum number of release sites (N_{min}) at the endbulb of Held synapses using variance-mean analysis. Mean release was varied using different extracellular Ca^{2+} concentrations (see Methods). As shown in Fig. 3, the estimated P_r at 2 mM [Ca^{2+}] was not significantly different between mature (0.54, SD 0.10; $n = 5$) and old mice (0.57, SD 0.10; $n = 5$) (unpaired t test: $t_8 = 0.474$, $P = 0.648$). There was no significant difference either in the estimated N_{min} between the two age groups (mature: 69 sites, SD 42, $n = 5$; old: 69 sites, SD 49, $n = 5$; unpaired t test: $t_8 = 0.0074$, $P = 0.994$). The similar estimate of P_r and N_{min} between mature and old mice is consistent with the observation that synapses in both age groups show similar quantal (Fig. 2*A–D*) and single-stimulus evoked synaptic transmission (Fig. 2*E*, *F*), and PPR (Fig. 2*H*, *I*). Together these observations suggest that synaptic transmission during the quiescent state remains unchanged during ageing at the endbulb of Held synapse in CBA/CaJ mice. It is worth noting that in a different mouse model of early onset ARHL, the DBA/2J mouse (Johnson *et al.* 2008), P_r was significantly reduced with concurrently enhanced PPR during hearing loss at the age of ∼45 days (Wang & Manis, 2005). This suggests that different mechanisms of synaptic transmission are affected by the hearing loss of these two different mouse strains.

Synaptic transmission during high-rate repetitive stimulation

Auditory nerve fibres can fire at sustained rates up to at least 450 Hz for environmentally relevant sound levels in cat (Kiang *et al.* 1965; Wen *et al.* 2009) and mouse (Taberner & Liberman, 2005). To examine how release at the endbulbs changes during high rates of afferent firing, we stimulated the nerve with 50-pulse stimulus trains at 100 and 400 Hz. At 100 Hz, every presynaptic stimulus evoked a reliable and precisely timed eEPSC in bushy neurons in both mature (Fig. 4*A*) and old (Fig. 4*B*) mice. At 400 Hz, release was maintained in mature mice, although with greater depression than at 100 Hz (Fig. 4*C*). However, in old mice, phasic release decreased part way through the 400 Hz train (Fig. 4*D*). The eEPSCs during the last 30 pulses of the train in old mice showed both reduced peak amplitudes and an increase in asynchronous events (Fig. 4*D*). The asynchronous events continued for tens of milliseconds after the end of the stimulus. To illustrate the kinetics of the synaptic depression, we measured the peak amplitudes of eEPSCs throughout the train, normalized to the first eEPSC (Fig. 4*E*). Steady state depression was quantified by averaging the normalized amplitude of the last 30 eEPSCs of the train. As shown in Fig. 4*F*, the steady state depression of eEPSC peak amplitude at 100 Hz showed no significant difference between mature (0.48, SD 0.12, $n = 12$) and old (0.51, SD 0.15, $n = 9$) mice (unpaired t test: $t_{19} = 0.481$, $P = 0.636$). At 400 Hz, the eEPSC peak amplitude was significantly more depressed during the steady state in old mice (mature: 0.18, SD 0.07, $n = 13$; old: 0.10, SD 0.06, $n = 9$; unpaired t test: $t_{20} = 2.618$, $P = 0.0165$). To investigate asynchronous release (Fig. 4*D*), we measured the charge transferred within each response window as the integrated area under each eEPSC, throughout the 50-pulse stimulus trains, and normalized this measure by the charge of the first eEPSC in the train (Fig. 4*G*). Steady state depression was again quantified by averaging the normalized eEPSC charge of the last 30 eEPSCs of the train. As shown in Fig. 4*H*, eEPSC charge in young and old mice depressed to similar levels during the trains at both 100 Hz (mature: 0.53, SD 0.11, $n = 12$; old: 0.57, SD 0.12, $n = 9$; unpaired t-test: $t_{19} = 0.796$, $P = 0.436$) and 400 Hz (mature: 0.32, SD 0.10, $n = 13$; old: 0.32, SD 0.12, $n = 9$; unpaired t-test: $t_{20} = 0.0579$, $P = 0.954$). At both rates, the accumulated charge throughout the trains was not significantly different between mature and old mice (100 Hz mature: 102 nA.ms, SD 53, $n = 12$; 100 Hz old: 77 nA.ms, SD 35, $n = 9$; unpaired t-test: $t_{19} = 1.242$, $P = 0.229$; and for 400 Hz mature: 47 nA.ms, SD 21, $n = 13$; 400 Hz old: 42 nA.ms,

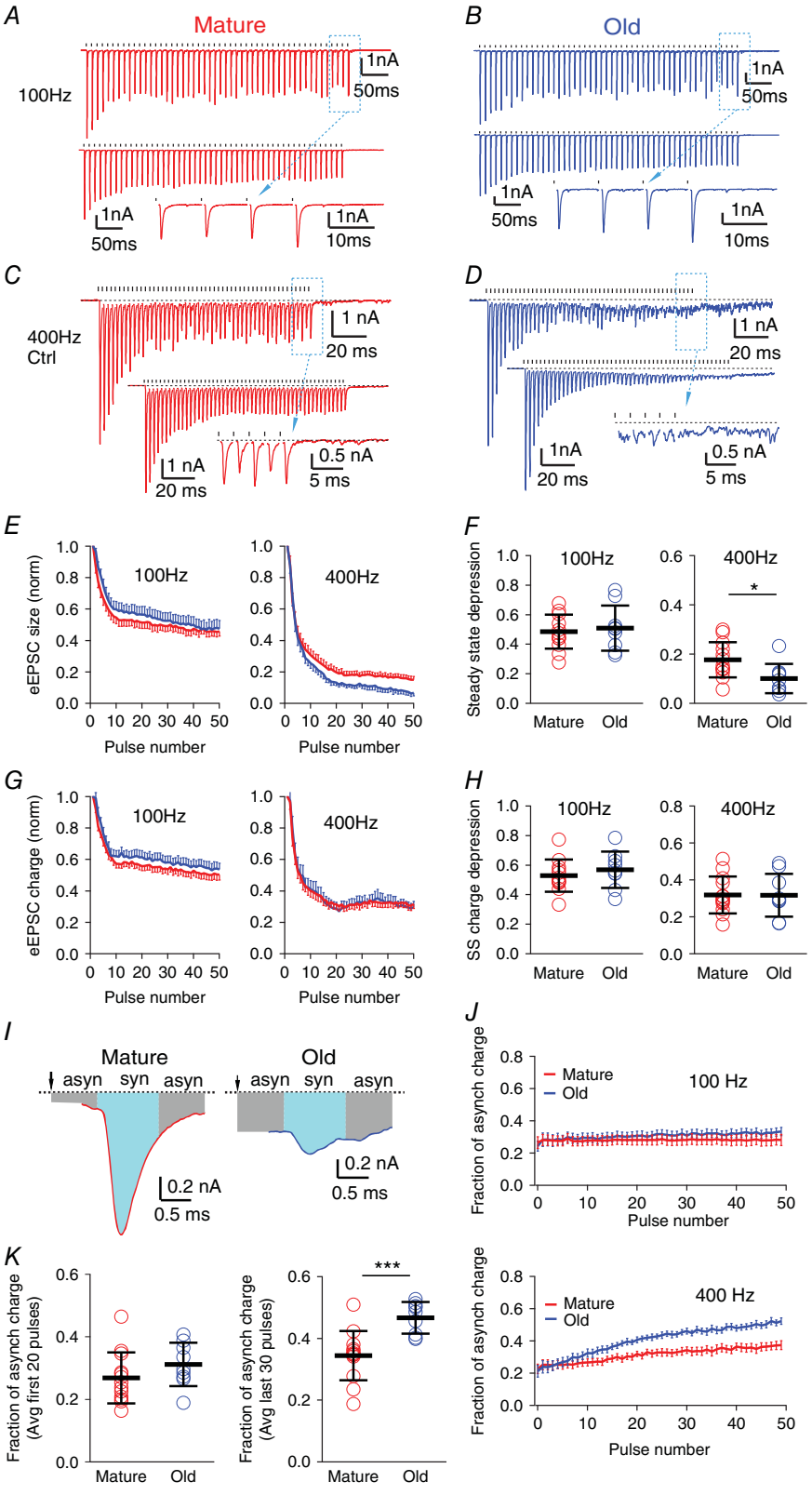

Figure 4. Asynchronous release is increased during high frequency stimulation in old mice
A, eEPSCs of a bushy neuron from a mature mouse in response to a 50-pulse stimulus train at 100 Hz. Top: single trial; bottom: average trace of 10 trials; inset: expanded view of the last eEPSCs from the dashed box in the top trace. Ticks above the traces mark stimulation times; dashed lines indicate the resting current. Plots in *B–D* are arranged the same way as in *A*. *B*, eEPSCs of a bushy neuron from an old mouse in response to a 50-pulse stimulus train at 100 Hz. *C* and *D*, eEPSCs of bushy neurons from mature (*C*) and old (*D*) mice in response to 50 pulse-trains at 400 Hz. Notice in *D* that eEPSCs show reduced peak amplitude and increased asynchronous release during the late part of the train. *E*, eEPSC peak amplitude throughout the stimulus train, normalized to the amplitude of the first eEPSC, at 100 and 400 Hz. *F*, summary of the steady state depression (average peak amplitude of the last 30 eEPSCs of the train normalized to the first eEPSC) at 100 and 400 Hz. Each symbol represents an individual neuron. *G*, eEPSC charge (integrated area under each eEPSC) throughout the stimulus train normalized to the charge of the first eEPSC, at 100 and 400 Hz. *H*, summary of the steady state (SS) charge depression (average charge of the last 30 eEPSCs of the train normalized to the first eEPSC) at 100 and 400 Hz. *I*, the last eEPSCs from the 400 Hz train in *C* (mature) and *D* (old). Syn: synchronous eEPSC response (cyan area); asyn: asynchronous eEPSC response (grey area). *J*, fraction of asynchronous release charge for each stimulus throughout the 50-pulse train at 100 Hz (top) and 400 Hz (bottom). *K*, average fraction of asynchronous charge of the first 20 stimuli (left) and the last 30 stimuli (right) of the 400 Hz trains in all bushy neurons. Data in *E*, *G* and *J* are presented as mean ± SEM; data in *F*, *H* and *K* are presented as mean ± SD . $^{*}P < 0.05$, $^{***}P < 0.001$.

SD 16, $n = 9$; unpaired t-test: $t_{20} = 0.689$, $P = 0.499$). These results suggest that the total release during the stimulus trains does not change between mature and old mice, and the eEPSC charge is depressed with similar kinetics throughout the trains at both 100 and 400 Hz (Fig. 4*G*, *H*). Therefore, the greater depression of eEPSC peak amplitude in old mice at 400 Hz (Fig. 4*E*, *F*), which was accompanied by an increase in asynchronous events (Fig. 4*D*), represents a shift in vesicle release from synchronous to asynchronous modes during high afferent firing rates.

To quantify the shift of vesicle release from synchronous to asynchronous during the stimulus train, we defined synchronous and asynchronous portions of each stimulus response. As shown in Fig. 4*I*, 'synchronous release' was defined as the charge occurring in a 1 ms window surrounding the eEPSC peak (0.4 ms before and 0.6 ms after), and 'asynchronous release' was defined as the remainder of the charge between successive stimuli (e.g. over the remaining 9.0 ms within a stimulus cycle for 100 Hz and 1.5 ms for 400 Hz, respectively). The fraction attributed to asynchronous release was consistent after the first few stimuli throughout the 50-pulse train at 100 Hz in both mature and old mice (Fig. 4*J*). Across the entire 100 Hz train, asynchronous response accounts for 28.1% (SD 10.7%, $n = 12$) of the total response in mature mice and 30.8% (SD 7.9%, $n = 9$) in old mice (unpaired t-test: $t_{19} = 0.64$, $P = 0.528$). During the first 20 pulses of the 400 Hz train (Fig. 4*J*, *K*), asynchronous release accounts for 26.9% (SD 8.2%, $n = 13$) of the charge in mature mice and 31.2% (SD 6.9%, $n = 9$) in old mice (unpaired t-test: $t_{20} = 1.30$, $P = 0.208$). However, the asynchronous release increased significantly during the last 30 pulses of the train in old mice (old: 46.7%, SD 5.1%, $n = 9$, mature: 34.4%, SD 8.0%, $n = 13$; unpaired t-test: $t_{20} = 4.06$, $P = 0.0006$). Conversely, the magnitude of synchronous release is substantially diminished at old synapses when challenged with sustained high frequency presynaptic firing rates (Fig. 4*E*, right panel), which is expected to reduce the temporal precision of synaptic transmission at the endbulb synapses.

To investigate whether there were different sizes of readily releasable vesicle pools (RRPs) at the endbulb of Held, using eEPSCs to 100 and 400 Hz stimulus trains, we used two different analyses of the responses to stimulus trains. First, eEPSC peak amplitudes in 100 Hz trains were measured to calculate the total quantal content of the RRP (Fig. 5*A*) using the method described by Schneggenburger *et al.* (1999). For each cell, the number of vesicles released for every stimulus was calculated by dividing the eEPSC peak amplitude by the average amplitude of sEPSC events for that neuron. The portion of the cumulative plot with steady state release (from the 11th to the 50th stimulus) was fit to a line, and back-extrapolated to time 0 to obtain the estimated RRP. There was no significant difference in RRP size between mature (193 vesicles, SD 74, $n = 11$) and old mice (167 vesicles, SD 57, $n = 9$) (Fig. 5*A*, right panel; unpaired t-test: $t_{18} = 0.844$, $P = 0.410$). We then performed the same analysis for EPSCs in the 400 Hz train. However, because 400 Hz trains evoked more asynchronous responses in old mice (Fig. 4*D*), we measured the total charge associated with each response in the time between stimuli (Fig. 5*B*). The estimated number of vesicles released at each stimulus was then calculated by dividing the eEPSC charge by the average charge of sEPSC events for that neuron. Again, no significant difference was found in the RRP size between mature (317 vesicles, SD 163, $n = 12$) and old mice (293 vesicles, SD 119, $n = 9$) (Fig. 5*B* right panel; unpaired t-test: $t_{19} = 0.367$, $P = 0.718$).

Second, we estimated the RRP size from both 100 and 400 Hz trains using the method of Elmqvist & Quastel (1965) (Fig. 5*C*, *D*). Individual evoked response amplitudes were plotted against the cumulative release that occurred prior to the given stimulus. Assuming that there is a minimum of new vesicle recruitment during the early part of the stimulus train, RRP size is estimated from the x-axis intercept of a line fit to responses to the first few stimuli (Fig. 5*C, D*). Again, the estimated RRP size was not significantly different between mature and old mice from either 100 Hz trains (Fig. 5*C*; mature: 628 vesicles, SD 350, $n = 12$; old: 727 vesicles, SD 645, $n = 9$; Mann–Whitney test: $P = 0.786$) or 400 Hz trains (Fig. 5*D*; mature: 280 vesicles, SD 152, $n = 12$; old: 268, SD 177, $n = 9$; Mann–Whitney test: $P = 0.633$). These estimates, which use different methods with distinct underlying assumptions, suggest that the RRP size of the endbulb of Held synapse is not different between mature and old mice. However, because of the assumptions behind these analyses, this should be viewed as a tentative conclusion (see Discussion).

Synchronous release in old mice can be restored with exogenous calcium buffering or by decreasing calcium influx

One hypothesis for the increase in asynchronous release is that during high rates of stimulation, calcium is not effectively cleared from the presynaptic terminal so that a buildup of presynaptic calcium triggers continued release of synaptic vesicles. The increase in this asynchronous release may also decrease the availability of docked vesicles for action potential evoked-release, leading to a decrease in synchronous release (Hagler & Goda, 2001). We therefore tested whether intraterminal calcium regulation might contribute to asynchronous release with two manipulations.

First, we pretreated the brain slices with 100 μM EGTA-AM (see Methods). Because EGTA is a 'slow' calcium buffer, it does not affect phasic release, but does provide additional calcium buffering at locations away from the calcium channels that directly drive phasic release

(Eggermann *et al.* 2012). In mature mice, pre-incubation of the slice in EGTA-AM did not change the single eEPSC peak amplitude (mature: −5.5 nA, SD 2.2, $n = 13$; mature+EGTA: −4.7 nA, SD 2.6, $n = 10$; unpaired t-test: $t_{21} = 0.8029$, $P = 0.431$), or the steady state depression of eEPSC amplitude in 400 Hz trains (Fig. 6*A*, *E*) (mature depression: 0.18, SD 0.07, $n = 13$; mature+EGTA depression: 0.20, SD 0.15, $n = 6$; Mann–Whitney test: $P = 0.999$). In old mice, EGTA-AM treatment also did not change the single eEPSC peak amplitude (old: −4.7 nA, SD 2.9, $n = 10$; old+EGTA: −3.4 nA, SD 2.5, $n = 9$; unpaired t-test: $t_{17} = 1.049$, $P = 0.309$). However, the EGTA-AM treatment reduced asynchronous release and enhanced synchronous release during the steady state response phase (Fig. 6*B* *vs.* 4*D*). Consequently, the steady state depression was significantly reduced (Fig. 6*B*, *E*) (old depression: 0.10, SD 0.06, $n = 9$; old+EGTA depression: 0.21, SD 0.07, $n = 7$; unpaired t-test: $t_{14} = 3.349$, $P = 0.0048$).

Second, we bath-applied 25 nM ω-agatoxin IVA to partially block P-type calcium channels, which should reduce action potential-evoked calcium influx into the endbulb terminal, and thus decrease calcium accumulation during sustained activity, while not completely blocking transmission. Consistent with a smaller calcium influx, the initial release was reduced with decreased single eEPSC peak amplitude (mature: −5.5 nA, SD 2.2, $n = 13$; mature+agatoxin: −0.8 nA, SD 0.7, $n = 7$; unpaired t-test: $t_{18} = 5.279$, $P < 0.0001$; old: −4.7 nA, SD 2.9, $n = 10$; old+agatoxin: −0.5 nA, SD 0.4, $n = 8$; unpaired t-test: $t_{16} = 3.932$, $P = 0.0012$). As expected for a decrease in calcium influx, the PPR of the first two eEPSCs of the 400 Hz train was significantly increased in both mature (Fig. 6*C*; control PPR: 0.90, SD 0.11; agatoxin PPR: 1.23, SD 0.16; $n = 7$; paired t-test: $t_6 = 4.22$, $P = 0.006$) and old mice (Fig. 6*D*; control PPR: 0.94, SD 0.22; agatoxin PPR: 1.25, SD 0.22; $n = 8$; paired t-test: $t_7 = 4.55$, $P = 0.003$). However, ω-agatoxin IVA did not change the relative amount of synchronous release during the sustained activity in mature mice (Fig. 6*C*). In old mice, ω-agatoxin IVA reduced asynchronous release and

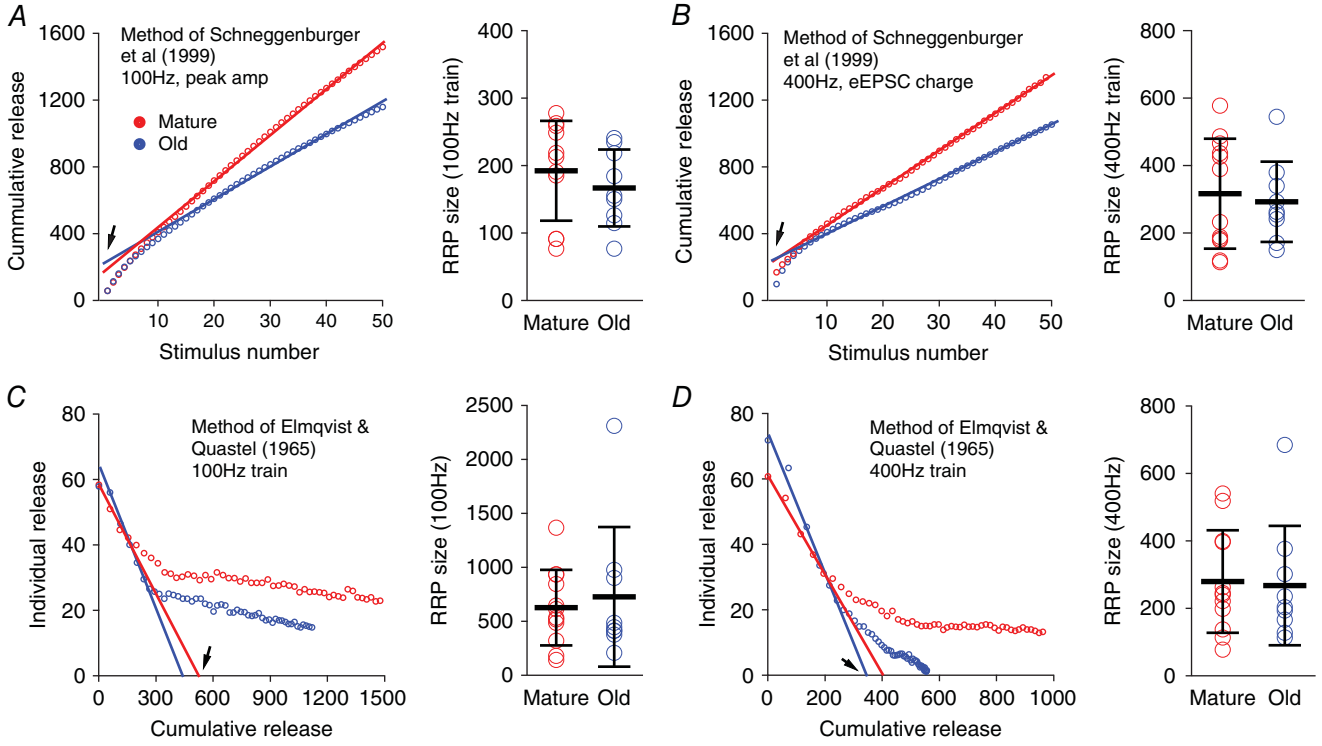

Figure 5. Estimates of RRP size in mature and old mice
A, RRP sizes calculated in two example endbulb synapses based on the cumulative plot of eEPSC peak amplitude using 100 Hz stimulus trains using the method of Schneggenburger *et al.* (1999). Circles: cumulative release in vesicle numbers against stimulus number; lines: line fit to the later points of the cumulative trace (stimulus number 11–50). The *y*-axis intercept (arrow) of the lines provides an estimate of the RRP size. Right panel: summary of RRP sizes in mature and old mice based on 100 Hz trains. *B*, RRP sizes calculated in two example endbulb synapses based on the cumulative plot of eEPSC charge using 400 Hz stimulus trains. Right panel: summary RRP sizes in mature and old mice based on 400 Hz trains. *C*, plots of the individual stimulus-evoked release against corresponding cumulative release that occurred prior to the given stimulus. RRP size is estimated from the *x*-axis intercept (arrow) of the fitted line to the early part of the stimulus train (method of Elmqvist & Quastel, 1965). Right panel: summary of the RRP size estimates from 100 Hz trains. *D*, as in *C* except using 400 Hz trains.

partially restored synchronous release (Fig. 6*D vs.* 4*D*). As shown in Fig. 6*F*, the average fraction of asynchronous release during the first 20 pulses of the 400 Hz train was not different between control, EGTA-AM treated and ω-agatoxin IVA treated slices in mature mice [mature control: 26.9% (SD 8.2%, $n = 13$); mature EGTA-AM: 25.0% (SD 10.9%, $n = 6$); mature ω-agatoxin IVA: 25.7% (SD 10.4%, $n = 7$); one-way ANOVA: $F_{2,23} = 0.0893$, $P = 0.915$], nor was it different in old mice [old control: 31.2% (SD 6.9%, $n = 9$); old EGTA-AM: 31.6% (SD 9.1%, $n = 7$); old ω-agatoxin IVA: 30.1% (SD 9.0%, $n = 8$); one-way ANOVA: $F_{2,21} = 0.0732$, $P = 0.930$]. During the last 30 pulses, the asynchronous response was also not different in mature mice [mature control: 34.4% (SD 8.0%, $n = 13$); mature EGTA-AM: 28.2% (SD 11.0%, $n = 6$); mature ω-agatoxin IVA: 31.6% (SD 9.3%, $n = 7$); one-way ANOVA: $F_{2,23} = 0.997$, $P = 0.384$]. However, both treatments significantly decreased asynchronous release during the last 30 stimuli in the train in old mice [old control: 46.7% (SD 5.1%, $n = 9$); old EGTA-AM: 36.3% (SD 11.2%, $n = 7$); old ω-agatoxin IVA: 37.1% (SD 7.6%, $n = 8$); one-way ANOVA: $F_{2,21} = 4.342$, $P = 0.0264$; Dunnett's multiple comparisons test: $P < 0.05$ between control and old EGTA-AM treatment, and between control and ω-agatoxin IVA treatment]. These results support the hypothesis that changes in intraterminal calcium handling in the endbulb of Held underlie the increased asynchronous release in mice with ARHL. It is also possible that there is a change in the calcium sensitivity of other mechanisms in the release process.

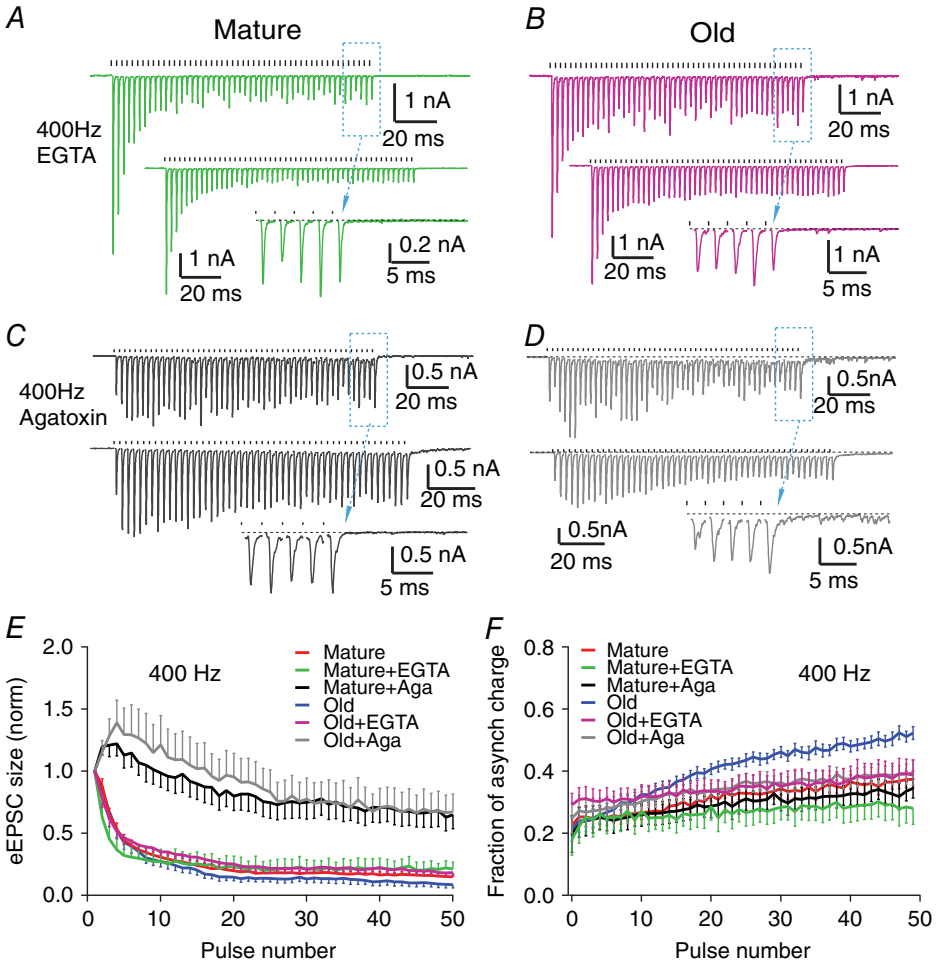

Figure 6. Synchronous synaptic transmission at 400 Hz is rescued by manipulations that decrease intraterminal calcium
A and *B*, eEPSCs in response to 400 Hz stimulus trains after treatment with EGTA-AM in mature (*A*) and old (*B*) mice. Top: single trial; bottom: average trace of 10 trials; inset: expanded view of the last eEPSCs from the dashed box in the top trace. Ticks above the trace mark stimulation times. Plots in *C* and *D* are arranged in the same format. *C* and *D*, eEPSCs in response to 400 Hz stimulus trains after bath application of 25 nM ω-agatoxin IVA in mature (*C*) and old (*D*) mice. *E*, normalized eEPSC peak amplitude to the first eEPSC throughout the stimulus trains at 400 Hz. *F*, fraction of asynchronous release charge throughout the 50-pulse trains at 400 Hz. EGTA: EGTA-AM treatment; Aga: ω-agatoxin IVA treatment. Data in *E* and *F* are shown as mean ± SEM.

Recovery from rate-dependent synaptic depression is faster in old mice

The rate of recovery in EPSC amplitude after depression by high-frequency stimulus trains depends on presynaptic calcium levels achieved during the stimulus train. Higher calcium levels produced by high-frequency stimuli have been shown to lead to a faster recovery of the release process (Wang & Kaczmarek, 1998; Wang & Manis, 2008). We assessed the recovery of eEPSC peak amplitude at the endbulb of Held by presenting 50-pulse stimulus trains followed by single test pulses with delays of 20, 70, 200, 500 or 1000 ms (Fig. 7*A*, *B*). The EPSC recovery was significantly faster in old mice than in the mature mice after both 100 Hz stimulus trains (Fig. 7*C*; mature: $n = 13$, old: $n = 10$; two-way ANOVA, age effect: $F_{1,84} = 8.93$, $P = 0.0037$; post-train delay time effect: $F_{3,84} = 4.50$, $P = 0.0056$; interaction: $F_{3,84} = 0.199$, $P = 0.897$) and 400 Hz stimulus trains (Fig. 7*D*; mature: $n = 13$, old: $n = 8$; two-way ANOVA, age effect: $F_{1,76} = 6.94$, $P = 0.0102$; delay time effect: $F_{3,76} = 4.39$, $P = 0.0067$; interaction: $F_{3,76} = 0.770$, $P = 0.515$). We also tested EPSC recovery following EGTA-AM pre-incubation. After a 100 Hz stimulus train (Fig. 7*C*), synapses in slices from mature mice pretreated with EGTA-AM did not differ from controls in their post-train recovery ($n = 6$; two-way ANOVA, EGTA-AM effect: $F_{1,68} = 2.78$, $P = 0.100$; delay time effect: $F_{3,68} = 5.21$, $P = 0.0027$; interaction: $F_{3,68} = 0.0277$, $P = 0.994$). EGTA-AM similarly had little effect in old mice for 100 Hz trains ($n = 5$; two-way ANOVA, EGTA-AM effect: $F_{1,52} = 2.14$, $P = 0.150$; delay time effect: $F_{3,52} = 1.88$, $P = 0.144$; interaction: $F_{3,52} = 0.00812$, $P = 0.999$). However, following a 400 Hz train (Fig. 7*D*), EPSC recovery in EGTA-AM treated slices was significantly slower in both mature mice ($n = 5$; two-way ANOVA, EGTA-AM effect: $F_{1,64} = 19.4$, $P < 0.0001$; delay time effect: $F_{3,64} = 7.64$, $P = 0.0002$; interaction: $F_{3,64} = 1.09$, $P = 0.360$) and old mice ($n = 5$; two-way ANOVA, EGTA-AM effect: $F_{1,44} = 5.49$, $P = 0.024$; delay time effect: $F_{3,44} = 2.37$, $P = 0.083$; interaction: $F_{3,44} = 0.225$, $P = 0.879$). The faster rate of recovery in old mice, and the return of the recovery time course following EGTA-AM pre-treatment towards that seen in mature mice, is also consistent with the hypothesis that the endbulb of Held synapses in old mice have an elevated intraterminal calcium level relative to mature mice during high rates of afferent firing. However, age-related changes in the expression of calcium binding proteins, or the sensitivity of calcium sensors that participate in synaptic transmission cannot be excluded.

Discussion

We compared synaptic transmission at the endbulb of Held synapses between mature and old CBA/CaJ mice. No significant difference was found at the endbulbs between two age groups of mice in the basal synaptic conductance amplitude and time course, the size of the RRP or the initial release probability. In old mice with ARHL, synaptic transmission at the endbulb synapse

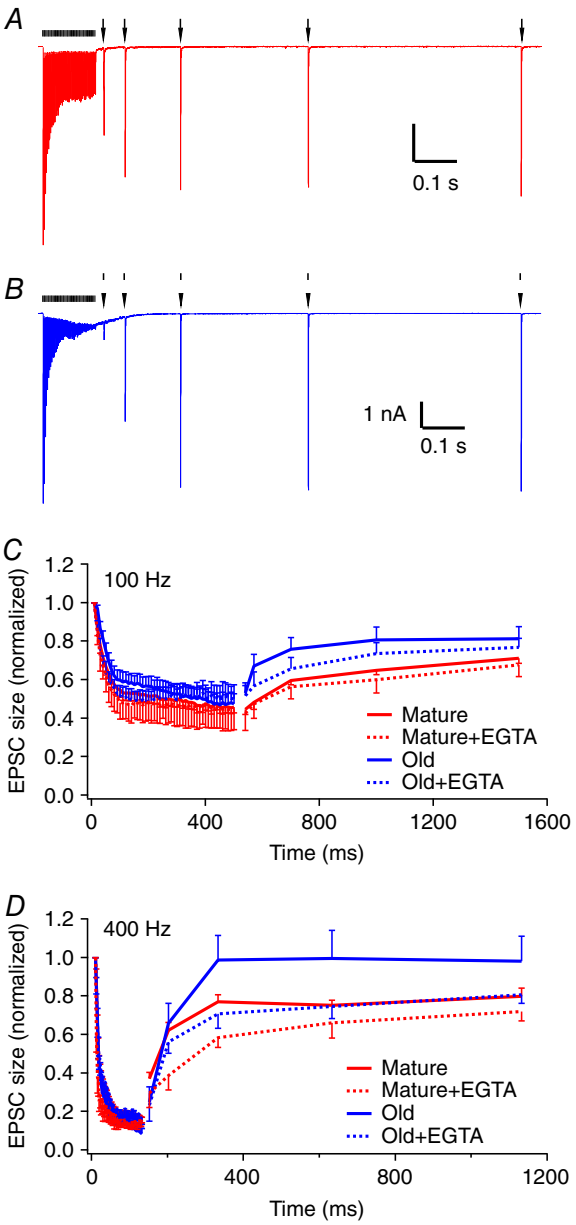

Figure 7. Recovery of eEPSC amplitude after the termination of stimulus trains is faster in old mice
A, eEPSCs (marked by arrows) from a mature mouse recover in amplitude after 50-pulse train at 400 Hz (marked by ticks). *B*, post-train eEPSC recovery in an old mouse. Traces are averages of five trials. *C*, summary of normalized eEPSC amplitudes for 100 Hz trains under control (continuous lines) and EGTA-AM treatment (dashed lines). *D*, dummary of eEPSC amplitudes for 400 Hz trains under control (continuous lines) and EGTA-AM treatment (dashed lines). Data are shown as mean ± SEM.

appears to function normally at low firing rates, but was unable to support sustained, time-locked transmission at high firing rates. Instead, synchronous release was decreased at high rates whereas asynchronous release was increased. Furthermore, manipulations that either increase intraterminal calcium buffering or decrease action potential-evoked calcium influx could restore the synchronous release while suppressing asynchronous release in response to high frequency afferent stimulation. These results suggest that endbulb synapses in old mice either have decreased capacity for buffering or clearing calcium in the terminal, increased action potential-triggered calcium influx, or that there is a change in the sensitivity of the calcium-dependent process involved in release.

ARHL and synaptic drive

Determining the proximal causes of the changes in synaptic transmission that we observed in old mice requires consideration of the nature of ARHL. CBA/CaJ mice with ARHL exhibit a loss of synapses between the hair cells and SGCs, and the loss is highly correlated with the amplitude of the first wave of the ABR (Sergeyenko *et al.* 2013), suggesting that synaptopathy is involved in the hearing loss. Aged CBA/CaJ mice also exhibit a loss of outer hair cells, which would also be expected to raise thresholds (Ohlemiller *et al.* 2010; Sergeyenko *et al.* 2013). On the other hand, there is little evidence in this strain for age-related changes in the endocochlear potential or sound transmission through the ossicular chain (Rosowski *et al.* 2003; Sha *et al.* 2008; Ohlemiller *et al.* 2010). Thus, the primary causes of ARHL in the CBA/CaJ mice appear to be limited to loss of hair cells and synapses onto SGCs. Because SGCs in the adult usually receive input from a single inner hair cell (Spoendlin, 1985; Berglund & Ryugo, 1987), the loss of hair cells and their connectivity with SGCs is expected to abolish both the sensory-evoked and spontaneous firing in affected SGCs. Thus, from the perspective of both spontaneous and acoustically driven action potentials, the subset of endbulb terminals that are disconnected from the periphery will experience an extended period of quiescence, including possible absence of spontaneous activity, with ageing. It is conceivable that there is a homeostatic compensation in the electrical excitability that leads to the generation of spontaneous spikes in the SGCs following hearing loss, but there is no evidence that this occurs. In addition, acoustic thresholds for driving the remaining SGCs will increase with the loss of outer hair cells, which over a lifetime of sound exposure would be expected to decrease the average firing rates and demands on release at the endbulb synapse, although spontaneous activity may be retained. Because the SGCs degenerate at a very slow rate, a large fraction (60% in CBA mice by ∼34 months) is preserved during ageing (Makary *et al.* 2011; Sergeyenko *et al.* 2013). For the surviving SGCs, their endbulb synapses also remain and continue to function, although activity-dependent mechanisms within the synapse may exhibit homeostatic adjustments in response to the lower levels of activity.

Because not all SGCs are disconnected from their hair cells during ARHL, there should be a substantial population of auditory nerve fibres and endbulb synapses that continue to have spontaneous activity and some level of acoustically driven activity. If the changes in transmission that we observe are solely dependent on sensory activity, then we might expect that there are two populations of endbulb synapses. However, there is no clear evidence in our data for a segregation of the aged synapses into two groups, one with normal, strong synchronous release and another with more asynchronous release, when tested at 400 Hz (Fig. 4*K*). This suggests that the factors leading to elevated asynchronous release are generalized across all endbulb synapses, and are at least somewhat independent of the status of the parent SGC.

It is interesting that evoked responses could not be achieved in 23% of the bushy cells from old mice. It is possible that this is an experimental artifact, and that the auditory nerve inputs onto these cells simply were not activated by the stimulating electrode. However, this rarely occurs for cells in slices from mature mice. It is also possible that these bushy cells have lost their auditory nerve inputs from SGCs. The loss of endbulbs would be consistent with the low sEPSC frequencies in these cells (Fig. 2*B*) when compared to the other bushy cells with evoked responses. Unfortunately, our sample size is too small to clearly distinguish these possibilities, and a morphological assay for the presence of endbulbs on these silent cells would be needed to provide convincing evidence for a loss of inputs.

Finally, we should consider whether the effects we have seen might arise from changes in the excitability of SGCs and their central axons. The auditory system operates with high firing rates under physiological conditions. Auditory nerve fibres fire spontaneously (in silence) at rates up to about 100 Hz, and in response to sound rates can increase to above 450 Hz (Kiang *et al.* 1965; Taberner & Liberman, 2005; Wen *et al.* 2009). Our results indicate that synaptic transmission at the endbulb synapse in aged mice is relatively normal at 100 Hz, which is within the range of spontaneous activity and firing rates in response to moderate levels of sound. However, at the upper end of the operating firing rate range (tested at 400 Hz), the aged endbulbs of Held are not capable of sustained release. This is unlikely to be caused by a failure of action potential initiation in aged SGCs, as eEPSC trains at 400 Hz in aged mice could be rescued by acute EGTA-AM treatment or partial block of voltage gated calcium channels (Fig. 6), and neither of these manipulations would be expected to

significantly affect the ability to initiate or sustain action potential initiation during a train.

RRP size of the endbulb of Held in mature and old mice

The calculation of readily release pool size with different methods using eEPSC trains did not show any significant differences between mature and old mice groups (Fig. 5), consistent with the observation of similar spontaneous event amplitudes and rates, and the amplitudes of single evoked synaptic events at both ages (Fig. 2). However, the RRP estimates using these analyses are dependent upon certain assumptions about the mechanisms involved in synaptic transmission (Neher, 2015). For example, the method of Schneggenburger *et al.* (1999) used in Fig. 5*A* and *B* assumes that the stimulus train reaches a steady state in which the vesicle release is balanced by recruitment of new vesicles. This assumption may not be met in aged mice, especially at 400 Hz, where it is not clear if new vesicles are reliably replenished to the RRP to balance released vesicles during the trains. By using long stimulus trains (11th to 50th pulses in Fig. 5*A*, *B*) we attempted to better reach a steady state of release in old mice, which should improve the reliability of RRP estimates with this method. The method of Elmqvist & Quastel (1965) used in Fig. 5*C* and *D* utilizes only early eEPSCs in the train, and assumes that there is little or no new vesicle recruitment during that period. However, at different activity rates, 100 and 400 Hz in this case, different levels of new vesicle recruitment might occur. At 100 Hz, the first four eEPSCs occur over 30 ms whereas the same four eEPSCs are complete in 7.5 ms for the 400 Hz train. We have no independent measure of new vesicle recruitment rates and those rates might differ at different release frequencies. Thus, these RRP estimates are probably rate-specific, and this may explain the differences in the RRP estimate between 100 Hz (Fig. 5*C*) and 400 Hz (Fig. 5*D*) trains from the same neurons.

Calcium signalling at the endbulb of Held synapses

Intracellular calcium dysregulation has long been postulated to underlie brain ageing and age-related conditions like Alzheimer's disease (Khachaturian, 1994), and one consequence of changes in calcium handling can be a shift in calcium-dependent processes of exocytosis at synaptic terminals. Synchronous and asynchronous vesicle release are two different modes of exocytosis that often occur together during repetitive presynaptic stimulation (Hagler & Goda, 2001). Synchronous release is tightly regulated by the immediate evaluation of calcium within the nanometre domain surrounding the voltage gated calcium channels upon presynaptic action potential invasion (Eggermann *et al.* 2012). Asynchronous release is thought to be associated with a buildup of calcium ions in the micrometre domain of the synaptic terminal during repetitive stimulation. These two types of release might utilize different presynaptic calcium sensors (Bacaj *et al.* 2013), as synchronous release is associated with high calcium cooperativity, whereas asynchronous release is associated with low calcium cooperativity (Sun *et al.* 2007). Synchronous and asynchronous release appear to mobilize vesicles from the same RRP (Hagler & Goda, 2001; Otsu *et al.* 2004; Sun *et al.* 2007; Yang & Xu-Friedman, 2010), although other evidence suggests that separate pools may be involved (Wen *et al.* 2013; Kaeser & Regehr, 2014). Regardless, the shift from synchronous release to asynchronous release during high firing rates at the endbulb of Held in old mice is consistent with the general hypothesis that calcium regulation is impaired during ageing in the CNS. During the post-train transmission, the rapid recovery of eEPSC peak amplitudes in old mice (Fig. 7) with simultaneously diminished asynchronous release suggests a quick switch between asynchronous and synchronous modes. Assuming both forms of release compete for the same RRP, the time course of the asynchronous release reduction presumably resembles the recovery kinetics of synchronous release.

The results from intraterminal calcium manipulations further support the idea that there is a change in calcium handling or calcium sensitivity at the endbulb synapses in aged mice. EGTA-AM treatment largely restored the phasic component of synaptic transmission at the endbulbs in old mice to a state closer to that of the mature mice (Fig. 6*B*, *F*). This result can be interpreted in two ways. First, it is possible that the intraterminal calcium concentration is abnormally elevated when challenged with high-rate stimuli during ageing. During high-rate stimulus trains, calcium builds up in the terminal (Habets & Borst, 2005), and is removed from the presynaptic zones by several mechanisms, including plasma membrane calcium pumps, Na–Ca exchangers, uptake into the endoplasmic reticulum or endoplasmic reticulum-like structures and uptake into mitochondria (Rizzuto *et al.* 2000). An age-related decrease in the capacity or function of one or more of these calcium handling pathways could lead to an elevated intraterminal calcium during the stimulus train, drive release asynchronously, reduce the population of docked vesicles at any moment and thereby compromise the ability of synchronized calcium influx to mobilize stimulus-dependent exocytosis. Second, there could be shifts in the expression of specific proteins or associated subunits, or their microenvironment, involved in the release process that changes the calcium sensitivity of release. For example, synaptotagmin-2 and synaptotagmin-7 are two major calcium sensors that govern synchronous and asynchronous vesicle release, respectively (Sun *et al.* 2007; Xu *et al.* 2007; Wen *et al.* 2010; Bacaj *et al.* 2013; Kaeser & Regehr, 2014; Luo *et al.* 2015),

and are highly expressed in fast auditory synapses (Sun *et al.* 2007; Xiao *et al.* 2010). It is conceivable that an age-related upregulation of synaptotagmin-7 and/or downregulation of synaptotagmin-2 at the endbulb of Held synapse could lead to the observed shift in the synaptic transmission from synchronous to asynchronous release in old mice.

Interestingly, partially blocking the P/Q type calcium channels, which are important for release at the endbulb of Held (Oleskevich & Walmsley, 2002; Lin *et al.* 2011), also improved synchronized synaptic transmission in old mice (Fig. 6*D*, *F*). This is consistent with the idea that elevated intratermial calcium could also come from abnormally increased calcium influx through voltage gated calcium channels. During sustained activity, calcium influx through voltage gated calcium channels at the endbulb of Held in prehearing mice is facilitated during trains of action potentials (Lin *et al.* 2011), which would lead to enhanced calcium influx during the later phase of the stimulus train. In mature animals, however, calcium influx is likely to be depressive at the endbulb during action potential trains due to calcium channel inactivation, as shown at the calyx of Held in the medial nucleus of the trapezoid body (Forsythe *et al.* 1998). It is possible that a switch from calcium channel inactivation to facilitation, or a decrease in inactivation, at the endbulb of Held during ageing could lead to enhanced calcium influx during the action potential trains in old mice.

In summary, we have shown that the endbulb of Held cannot support synchronous release at high rates in aged mice with ARHL. This deficit may result from the global biological processes of ageing, or from the decrease in activity associated with sensory hearing loss. The results from experimental manipulations of intraterminal calcium are consistent with the hypothesis that the deficit results from a build up of intraterminal calcium during high frequencies of stimulation, but could also be explained by changes in the calcium sensitivity of proteins involved in the release process. Regardless, these experiments suggest that perceptual deficits associated with ARHL may in part result from an inability of the first central auditory synapses to reliably transmit the temporal information present in sound, as represented by the high firing rates and exceptional temporal precision of spikes in auditory nerve fibres.

References

Anderson S, Parbery-Clark A, White-Schwoch T & Kraus N (2012). Aging affects neural precision of speech encoding. *J Neurosci* **32**, 14156–14164.

Bacaj T, Wu D, Yang X, Morishita W, Zhou P, Xu W, Malenka RC & Sudhof TC (2013). Synaptotagmin-1 and synaptotagmin-7 trigger synchronous and asynchronous phases of neurotransmitter release. *Neuron* **80**, 947–959.

Berglund AM & Ryugo DK (1987). Hair cell innervation by spiral ganglion neurons in the mouse. *J Comp Neurol* **255**, 560–570.

Bohne BA, Gruner MM & Harding GW (1990). Morphological correlates of aging in the chinchilla cochlea. *Hear Res* **48**, 79–91.

Campagnola L, Kratz MB & Manis PB (2014). ACQ4: an open-source software platform for data acquisition and analysis in neurophysiology research. *Front Neuroinform* **8**, 3.

Caspary DM, Schatteman TA & Hughes LF (2005). Age-related changes in the inhibitory response properties of dorsal cochlear nucleus output neurons: role of inhibitory inputs. *J Neurosci* **25**, 10952–10959.

Clements JD & Bekkers JM (1997). Detection of spontaneous synaptic events with an optimally scaled template. *Biophys J* **73**, 220–229.

Eggermann E, Bucurenciu I, Goswami SP & Jonas P (2012). Nanodomain coupling between Ca^{2+} channels and sensors of exocytosis at fast mammalian synapses. *Nat Rev Neurosci* **13**, 7–21.

Elmqvist D & Quastel DM (1965). A quantitative study of end-plate potentials in isolated human muscle. *J Physiol* **178**, 505–529.

Forsythe ID, Tsujimoto T, Barnes-Davies M, Cuttle MF & Takahashi T (1998). Inactivation of presynaptic calcium current contributes to synaptic depression at a fast central synapse. *Neuron* **20**, 797–807.

Frisina DR & Frisina RD (1997). Speech recognition in noise and presbycusis: relations to possible neural mechanisms. *Hear Res* **106**, 95–104.

Frisina RD & Walton JP (2006). Age-related structural and functional changes in the cochlear nucleus. *Hear Res* **216–217**, 216–223.

Guimaraes P, Zhu X, Cannon T, Kim S & Frisina RD (2004). Sex differences in distortion product otoacoustic emissions as a function of age in CBA mice. *Hear Res* **192**, 83–89.

Habets RL & Borst JG (2005). Post-tetanic potentiation in the rat calyx of Held synapse. *J Physiol* **564**, 173–187.

Hagler DJ, Jr & Goda Y (2001). Properties of synchronous and asynchronous release during pulse train depression in cultured hippocampal neurons. *J Neurophysiol* **85**, 2324–2334.

Henry KR (2004). Males lose hearing earlier in mouse models of late-onset age-related hearing loss; females lose hearing earlier in mouse models of early-onset hearing loss. *Hear Res* **190**, 141–148.

Hequembourg S & Liberman MC (2001). Spiral ligament pathology: a major aspect of age-related cochlear degeneration in C57BL/6 mice. *J Assoc Res Otolaryngol* **2**, 118–129.

Johnson KR, Longo-Guess C, Gagnon LH, Yu H & Zheng QY (2008). A locus on distal chromosome 11 (ahl8) and its interaction with Cdh23 ahl underlie the early onset, age-related hearing loss of DBA/2J mice. *Genomics* **92**, 219–225.

Joris P & Yin TC (2007). A matter of time: internal delays in binaural processing. *Trends Neurosci* **30**, 70–78.

Kaeser PS & Regehr WG (2014). Molecular mechanisms for synchronous, asynchronous, and spontaneous neurotransmitter release. *Ann Rev Physiol* **76**, 333–363.

Khachaturian ZS (1994). Calcium hypothesis of Alzheimer's disease and brain aging. *Ann N Y Acad Sci* **747**, 1–11.

Kiang NY, Pfeiffer RR, Warr WB & Backus AS (1965). Stimulus coding in the cochlear nucleus. *Trans Am Otol Soc* **53**, 35–58.

Lin KH, Oleskevich S & Taschenberger H (2011). Presynaptic Ca^{2+} influx and vesicle exocytosis at the mouse endbulb of Held: a comparison of two auditory nerve terminals. *J Physiol* **589**, 4301–4320.

Lorenzi C, Gilbert G, Carn H, Garnier S & Moore BC (2006). Speech perception problems of the hearing impaired reflect inability to use temporal fine structure. *Proc Natl Acad Sci USA* **103**, 18866–18869.

Luo F, Bacaj T & Sudhof TC (2015). Synaptotagmin-7 is essential for Ca^{2+}-triggered delayed asynchronous release but not for Ca^{2+}-dependent vesicle priming in retinal ribbon synapses. *J Neurosci* **35**, 11024–11033.

Makary CA, Shin J, Kujawa SG, Liberman MC & Merchant SN (2011). Age-related primary cochlear neuronal degeneration in human temporal bones. *J Assoc Res Otolaryngol* **12**, 711–717.

Manis PB, Xie R, Wang Y, Marrs GS & Spirou GA (2011). The endbulbs of Held. In *Synaptic Mechanisms in the Auditory System*, ed. Trussell LO, Popper AN & Fay RR, pp. 61–93. Springer, New York.

Neher E (2015). Merits and limitations of vesicle pool models in view of heterogeneous populations of synaptic vesicles. *Neuron* **87**, 1131–1142.

Ohlemiller KK, Dahl AR & Gagnon PM (2010). Divergent aging characteristics in CBA/J and CBA/CaJ mouse cochleae. *J Assoc Res Otolaryngol* **11**, 605–623.

Oleskevich S, Clements J & Walmsley B (2000). Release probability modulates short-term plasticity at a rat giant terminal. *J Physiol* **524**, 513–523.

Oleskevich S & Walmsley B (2002). Synaptic transmission in the auditory brainstem of normal and congenitally deaf mice. *J Physiol* **540**, 447–455.

Otsu Y, Shahrezaei V, Li B, Raymond LA, Delaney KR & Murphy TH (2004). Competition between phasic and asynchronous release for recovered synaptic vesicles at developing hippocampal autaptic synapses. *J Neurosci* **24**, 420–433.

Reid CA & Clements JD (1999). Postsynaptic expression of long-term potentiation in the rat dentate gyrus demonstrated by variance-mean analysis. *J Physiol* **518**, 121–130.

Rizzuto R, Bernardi P & Pozzan T (2000). Mitochondria as all-round players of the calcium game. *J Physiol* **529**, 37–47.

Rosowski JJ, Brinsko KM, Tempel BI & Kujawa SG (2003). The aging of the middle ear in 129S6/SvEvTac and CBA/CaJ mice: measurements of umbo velocity, hearing function, and the incidence of pathology. *J Assoc Res Otolaryngol* **4**, 371–383.

Schneggenburger R, Meyer AC & Neher E (1999). Released fraction and total size of a pool of immediately available transmitter quanta at a calyx synapse. *Neuron* **23**, 399–409.

Schulte BA & Schmiedt RA (1992). Lateral wall Na,K-ATPase and endocochlear potentials decline with age in quiet-reared gerbils. *Hear Res* **61**, 35–46.

Sergeyenko Y, Lall K, Liberman MC & Kujawa SG (2013). Age-related cochlear synaptopathy: an early-onset contributor to auditory functional decline. *J Neurosci* **33**, 13686–13694.

Sha SH, Kanicki A, Dootz G, Talaska AE, Halsey K, Dolan D, Altschuler R & Schacht J (2008). Age-related auditory pathology in the CBA/J mouse. *Hear Res* **243**, 87–94.

Shofner WP (2008). Representation of the spectral dominance region of pitch in the steady-state temporal discharge patterns of cochlear nucleus units. *J Acoust Soc Am* **124**, 3038–3052.

Spoendlin H (1985). Anatomy of cochlear innervation. *Am J Otolaryngol* **6**, 453–467.

Sun J, Pang ZP, Qin D, Fahim AT, Adachi R & Sudhof TC (2007). A dual-Ca^{2+}-sensor model for neurotransmitter release in a central synapse. *Nature* **450**, 676–682.

Taberner AM & Liberman MC (2005). Response properties of single auditory nerve fibres in the mouse. *J Neurophysiol* **93**, 557–569.

Viana LM, O'Malley JT, Burgess BJ, Jones DD, Oliveira CA, Santos F, Merchant SN, Liberman LD & Liberman MC (2015). Cochlear neuropathy in human presbycusis: confocal analysis of hidden hearing loss in post-mortem tissue. *Hear Res* **327**, 78–88.

Wang LY & Kaczmarek LK (1998). High-frequency firing helps replenish the readily releasable pool of synaptic vesicles. *Nature* **394**, 384–388.

Wang Y & Manis PB (2005). Synaptic transmission at the cochlear nucleus endbulb synapse during age-related hearing loss in mice. *J Neurophysiol* **94**, 1814–1824.

Wang Y & Manis PB (2008). Short-term synaptic depression and recovery at the mature mammalian endbulb of Held synapse in mice. *J Neurophysiol* **100**, 1255–1264.

Wen B, Wang GI, Dean I & Delgutte B (2009). Dynamic range adaptation to sound level statistics in the auditory nerve. *J Neurosci* **29**, 13797–13808.

Wen H, Hubbard JM, Rakela B, Linhoff MW, Mandel G & Brehm P (2013). Synchronous and asynchronous modes of synaptic transmission utilize different calcium sources. *eLife* **2**, e01206.

Wen H, Linhoff MW, McGinley MJ, Li GL, Corson GM, Mandel G & Brehm P (2010). Distinct roles for two synaptotagmin isoforms in synchronous and asynchronous transmitter release at zebrafish neuromuscular junction. *Proc Natl Acad Sci USA* **107**, 13906–13911.

Xiao L, Han Y, Runne H, Murray H, Kochubey O, Luthi-Carter R & Schneggenburger R (2010). Developmental expression of synaptotagmin isoforms in single calyx of Held-generating neurons. *Mol Cell Neurosci* **44**, 374–385.

Xie R & Manis PB (2013*a*). Glycinergic synaptic transmission in the cochlear nucleus of mice with normal hearing and age-related hearing loss. *J Neurophysiol* **110**, 1848–1859.

Xie R & Manis PB (2013*b*). Target-specific IPSC kinetics promote temporal processing in auditory parallel pathways. *J Neurosci* **33**, 1598–1614.

Xu J, Mashimo T & Sudhof TC (2007). Synaptotagmin-1, -2, and -9: Ca^{2+} sensors for fast release that specify distinct presynaptic properties in subsets of neurons. *Neuron* **54**, 567–581.

Yang H & Xu-Friedman MA (2010). Developmental mechanisms for suppressing the effects of delayed release at the endbulb of Held. *J Neurosci* **30**, 11466–11475.
Zheng QY, Johnson KR & Erway LC (1999). Assessment of hearing in 80 inbred strains of mice by ABR threshold analyses. *Hear Res* **130**, 94–107.

Additional information

Competing interests

The authors have no competing financial interests to declare.

Author contributions

R.X. and P.B.M. designed the work. R.X. performed experiments and analysed data. R.X. and P.B.M. wrote the manuscript. Both R.X. and P.B.M. approved the final version of the manuscript and agree to be accountable for all aspects of the work in ensuring that questions related to the accuracy or integrity of any part of the work are appropriately investigated and resolved. Both R.X. and P.B.M. qualify for authorship, and there are no other qualified authors.

Funding

This work was supported by the US National Institute on Deafness and other Communication Disorders grants R03DC013396 (R.X.), R01DC004551 (P.B.M.), and the Deafness Research Foundation (now Hearing Health Foundation) research grant (R.X.).

Acknowledgements

We thank H. O'Donohue and S. Lin for experimental and organizational support, and H. O'Donohue and M. Kratz for comments on the manuscript.

Authors' translational perspective

We report that the first central auditory synapse, the endbulb of Held, has decreased synchronous transmitter release in aged mice for high rate stimuli, and that the deficit in release can be partially reversed by increasing the calcium buffering, or decreasing calcium influx, at the synapse. Whether this effect is age-related or activity-dependent is not clear at this point. These experiments suggest that perceptual deficits in ARHL may in part result from an inability of the first central auditory synapses to reliably transmit the fine temporal structure of activity in the auditory nerve at high rates. If translatable to humans, these observations suggest that using high rates of stimulation with cochlear implants, or strong amplification with hearing aids, that drive the residual auditory system at high rates, are likely to be counterproductive in terms of optimizing the transfer of information to the central auditory pathways, and in improving the ability to perceive and discriminate sounds. These experiments also point to potential mechanisms that could be manipulated to improve the fidelity of transmission at the endbulb of Held under these conditions.